Calculation of the Color Matching Functions of Digital Cameras from Their Complete Spectral Sensitivities

Francisco Martínez–Verdú▲
Departamento Interuniversitario de Óptica, Universidad de Alicante, Alicante, Spain

Jaume Pujol
Centro de Desarrollo de Sensores, Instrumentación y Sistemas (CD6), Universidad Politécnica de Cataluña (UPC), Terrassa, Barcelona, Spain

Pascual Capilla
Departamento de Óptica, Universidad de Valencia, Burjassot, Valencia, Spain

We propose a new algorithm to obtain the color matching functions of any digital camera, with correct weights and white balance, from the relative scaling of their complete (3-D) spectral sensitivities obtained from real spectroradiometric data. Thanks to this algorithm, it is possible to predict the RGB digital levels of any digital camera in realistic illumination-scene environments—spatially non-uniform illumination field, variable chromaticity and large dynamic range of luminance levels—opening the possibility of transforming any digital camera into a tele-colorimeter. The illumination-scene test was the Macbeth ColorChecker Chart under three different light sources (halogen, metal halide and daylight fluorescent lamps), provided by a non-standard light box. The results confirmed that it is possible to predict any RGB digital levels exclusively by varying the *f*–number of the camera zoom lens.

Journal of Imaging Science and Technology 46: 15–25 (2002)

Introduction

In digital color imaging it is necessary to know the spectral sensitivities of the color system or device in order to implement them in the colorimetric profile, which is inserted in the color reproduction chain, and the management of multimedia devices (capture, visualization and printing).[1–5] Thanks to this, acceptable color reproduction is obtained between the relative colorimetry of the real scene and the estimated colorimetric data in each of the different image types (RGB-capture, RGB-visualization, CMYK-printing).

The main problem with digital image capture devices (scanners and cameras) is controlling their raw RGB space. Although the basic components are always essentially the same—zoom lens, optoelectronic sensor (CCD, CMOS) and frame grabber—there are many variables, both optical (relative aperture or *f*-number, photosite integration time) and electronic (additional gain, matrixing, white balancing, gamma monitor, etc.), which can alter the true raw device RGB space. In the initial processing stages, any digital image capture device is an additive color reproduction system because the optoelectronic sensor captures or sums photons. Therefore its raw spectral sensitivities must all be positive.[6–8] However, when the raw RGB space is electronically varied, the resulting spectral sensitivities may have negative parts. This hinders the fundamental analysis of the color reproduction quality among apparently similar performances of different trademark devices. This subject is so important that ISO 17321[9] (Color characterization of digital cameras) proposes that the direct digital data, like RGB space, should not be matrixed except when they have been previously transformed using the following processes:

- linearization (if necessary);
- dark current/frame subtraction;
- shading & sensitivity (flat field) correction;
- flare removal (scene-dependent);
- white balancing (adopted white has neutral code values; i.e. equal RGB values or no chrominance);
- demosaicing (color pixel reconstruction).

Therefore, when we want to apply an algorithm (either empirical or model-based) to obtain the spectral sensitivities of a digital image capture system, we should be sure of what the RGB space of the device is, because any electronic variation of RGB data means a different set of spectral sensitivities. For instance, if the white balancing is changed electronically, the new spectral

Original manuscript received February 7, 2001

▲ IS&T Member

Color Plates 6 through 11 are printed in the color plate section of this issue, pp. 55–58.

sensitivities are not just a chromatic-adaptation transformation of the old sensitivities. The correct procedure should be to obtain the spectral sensitivity set again experimentally because the new raw RGB encoding is different from the old one.

Spectral Characterization Methods

The first approach is theoretical, educational and strictly optical because it is based on the color separation device, but it is difficult to apply in real cases. If we know the spectral characteristic of each component of the color architecture (3-CCD prism block, color stripe filters, etc.) beforehand, and also the effect of the electronic processing on color signals, we can estimate the spectral sensitivity set of the color device exactly. Taking as an example a 3-CCD digital camera (**Color Plate 6, p. 55**), the prior knowledge of the spectral transmittances of the zoom lens $\tau_{LENS}(\lambda)$, cut-off IR filter $\tau_{IR}(\lambda)$, dichroic prisms $\tau_1(\lambda)$, $\tau_2(\lambda)$, color filters $\tau_R(\lambda)$, $\tau_G(\lambda)$, $\tau_B(\lambda)$, and the spectral quantum efficiency $QE(\lambda)$ of the optoelectronic sensor, should allow us to establish that the spectral sensitivity set of the digital image capture system is:

$$\begin{aligned} s_R(\lambda) &\propto \tau_{LENS}(\lambda)\tau_{IR}(\lambda)\tau_1(\lambda)\left[1-\tau_2(\lambda)\right]\tau_R(\lambda)QE(\lambda) \\ s_G(\lambda) &\propto \tau_{LENS}(\lambda)\tau_{IR}(\lambda)\tau_1(\lambda)\tau_2(\lambda)\tau_G(\lambda)QE(\lambda) \\ s_B(\lambda) &\propto \tau_{LENS}(\lambda)\tau_{IR}(\lambda)\left[1-\tau_1(\lambda)\right]\tau_B(\lambda)QE(\lambda) \end{aligned} \quad (1)$$

In general, the manufacturers of digital image capture devices (scanners, cameras) use this optical approach as technical information for the user, but here issues such as the influence of the white balance on the final spectral sensitivities are not taken into account, so the raw RGB encoding is ambiguous. Therefore, it should be advantageous to change to another approach where the digital image capture device is considered as a "black box", some of whose processes on the color signals are controlled (such as the electronic white balance).

The spectroradiometric approach is based on this idea and consists essentially of obtaining the response or digital level DL_λ to a monochromatic stimulus with radiant energy $L_{e\lambda}$ (spectral radiance). The required basic experimental set-up consists of a light source, a monochromator and a radiance meter. The procedure for computing the spectral sensitivity set can be summarized from the ISO 17321 standard for digital still cameras (DSC). Monochromatic images, with wavelengths from 360 nm to 830 nm (1100 nm if necessary because the digital image capture device does not have a cut-off IR filter), in 10 nm steps, are captured by each color channel (i = R, G, B). Simultaneously, the digital level of each monochromatic image $DL_{\lambda i}$ is associated with the relative radiance $L_{e\lambda}/L_{e\lambda\,max}$. Additionally, the *OECFs* (optoelectronic conversion functions) are obtained for each color channel according to ISO 14524.[10] With these data and the monochromatic image set, the relative spectral sensitivity set is obtained as follows:

- Use the inverse alternative focal plane *OECF* to linearize the raw DSC response at each wavelength: $OECF_i^{-1}(DL_{\lambda i})$.
- Take the algorithm of the linearized DSC responses: $\log\,[OECF_i^{-1}(DL_{\lambda i})]$. Average a 64 × 64 pixel block of log values at the center of each image to determine the raw DSC log response at each wavelength. Take the antilog of the averaged log responses to determine the linearized DSC response at each wavelength: antilog (mean $\{\log\,[OECF_i^{-1}(DL_{\lambda i})]\}$).
- Calculate the relative spectral sensitivity set at each wavelength for each color channel by dividing the linearized DSC response by the relative radiance:

$$s_i(\lambda) = \frac{10^{-\text{mean}\left\{\log\left[OECF_i^{-1}(DL_{\lambda i})\right]\right\}}}{L_{e\lambda}/L_{e\lambda\,max}} \quad (2)$$

- Obtain the DSC spectral response values for each color channel at each wavelength, or color matching functions $\mathbf{T_{RGB}}$ by multiplying the relative spectral sensitivity set by the relative spectral power distribution $SPD(\lambda)$ of the monochromator lamp or other light source (if, for instance, the digital image capture device has its own lighting system).

$$\begin{aligned} \bar{r}(\lambda) &= \frac{10^{-\text{mean}\left\{\log\left[OECF_R^{-1}(DL_{\lambda R})\right]\right\}}}{L_{e\lambda}/L_{e\lambda\,max}} SPD(\lambda) \\ \bar{g}(\lambda) &= \frac{10^{-\text{mean}\left\{\log\left[OECF_G^{-1}(DL_{\lambda G})\right]\right\}}}{L_{e\lambda}/L_{e\lambda\,max}} SPD(\lambda) \\ \bar{b}(\lambda) &= \frac{10^{-\text{mean}\left\{\log\left[OECF_B^{-1}(DL_{\lambda B})\right]\right\}}}{L_{e\lambda}/L_{e\lambda\,max}} SPD(\lambda) \end{aligned} \quad (3)$$

$$\Rightarrow \mathbf{T_{RGB}} = \left[\bar{\mathbf{r}} \quad \bar{\mathbf{g}} \quad \bar{\mathbf{b}}\right]_{48\times 3}$$

- Normalize the spectral responses for each color channel by dividing by the constant necessary to make the sum of the spectral responses for each color channel equal to unity:

$$\bar{\mathbf{r}}^t \cdot \mathbf{E} = 1,\ \bar{\mathbf{g}}^t \cdot \mathbf{E} = 1,\ \bar{\mathbf{b}}^t \cdot \mathbf{E} = 1,$$

where $\mathbf{E} = [1, 1, ..., 1]^t$. ($\mathbf{A}^t$ is the transpose of matrix $\mathbf{A}$.)

This empirical approach is very similar to that used in the spectral characterization of TV cameras[11] or of internet videoconferences.[12] The basic formalism to determine the relative spectral sensitivity, such as the ratio between response and relative radiance, is the same. Nevertheless, some methodological aspects of the experimental set-up and the data post-processing hinder a direct comparison among three standards. For instance, with the IEC 61966-9 standard, the obtained relative spectral sensitivities have negative values at some wavelengths, which does not make colorimetric sense because they must be completely positive. This means that either the data processing is not taken at raw encoding level or the data post-processing brings about a serious colorimetric error.

The key to the success of the spectroradiometric approach is to control the radiant energy of the monochromatic stimulus. The energy should be the same for each wavelength; that is, we try to obtain the system response to an absolute equal energy stimulus **E** (in

W/sr·m²). Because we work with a real light source whose $SPD(\lambda)$ is not adjusted to the equal energy stimulus **E**, it seems necessary to use the term $L_{e\lambda}/L_{e\lambda\max}$ in order to control this. However, because the digital image capture devices are not strictly linear, the *OECFs* are previously determined and afterwards used (in inverse mode) to compensate for this effect. However, because the *OECFs* connect the digital levels DL_i with the photometric exposure H (lx·s) as described in ISO 14524,[10] when we run $OECF^{-1}(DL_{\lambda i})$ the radiometric units (W/sr·m²) are not obtained except for the photometric units (lx·s). Hence, meter sense is lacking in a photosensor system whose global spectral sensitivity (the envelope of the spectral sensitivities of the three color channels) is never adjusted to the photopic sensitivity curve V_λ, which is exclusive to the human visual system. It is therefore incongruent to impose *a priori* a V_λ-type spectral sensitivity on a digital image capture device whose spectral sensitivities are ruled strictly by radiometric and not photometric laws. Furthermore, as a final objection, when we impose a normalization algorithm for the color matching functions based on the equal energy stimulus **E**, it is assumed that the true (not the electronic) white balance should be 1:1:1. That is, the adapted white (**E**) coincides with the adopted white (by electronic control), but it is not possible to test this point due to the metameric nature of image capture. For instance, if we consider a digital still camera working under incandescent light (illuminant A, XYZ balance 1.0987:1:0.3559), the electronic white balance should be adjusted approximately to a $SPD(\lambda)$ with color temperature $T_C \sim 3000$ K. If we performed the final step of normalization of the color matching functions, we would be imposing *a posteriori* a white balance which is not fixed initially.

The third approach to the spectral characterization of digital image capture devices is strictly based on mathematical models. This mathematical approach is easily outlined using the vector notation in the colorimetry of a digital image capture device.[6–8,13] If **K** is a set of spectral reflectances $\rho(\lambda)$ (such as the ColorChecker chart), we can establish that the device responses are $\mathbf{t_{RGB}} = \mathbf{T_{RGB}}^{t} \cdot \mathbf{K}$. Therefore, an initial estimation of the color matching function $\mathbf{T_{RGB}}$ may be obtained with the Moore–Penrose pseudo-inverse method:

$$\mathbf{T_{RGB}} = \left(\mathbf{K} \cdot \mathbf{K}^{t}\right)^{-1} \cdot \mathbf{K} \cdot \mathbf{t_{RGB}}^{t} \tag{4}$$

From this equation, the classic estimation methods of Wiener[14,15] and others, which use constrained regression methods[16–18] or projections onto convex sets[19,20] can be described. When we consider real digital image capture devices, with noise, these estimations are unpredictable. This improves sufficiently, although it is highly dependent on the selection of the spectral reflectance set (by physical or statistical modeling), if the algebraic problem is approached by stating the principal components method by applying the singular value decomposition (SVD) to the matrix **K**.

Table I summarizes the advantages and disadvantages of these methods. The optical approach does not take into account the electronics of the device, but it is very instructive. The spectroradiometric approach is tedious, but it is realistic, without any decontrolled parameters. The mathematical approach is simple but inaccurate because it does not take into account the optoelectronics of the device.

TABLE I. Advantages and Disadvantages of the Spectral Characterization Methods

Approach	Advantages	Disadvantages
Optical	Educational	Ideal Device
Spectroradiometric	Real Device = Black Box	Tedious, Complicated
Mathematical	Computationally Easy	Ideal Device

Once the spectral sensitivity set of the digital image capture device is obtained, regardless of the method used, it is finally possible to calculate the color reproduction quality index by finding the similarity index between the color matching functions $\mathbf{T_{RGB}}$ and the CIE Standard Observer $\mathbf{T_{XYZ}}$, by the constrained regression[21] or projection onto convex sets[22] methods. Because the color matching functions $\mathbf{T_{RGB}}$ are not exact linear combinations of $\mathbf{T_{XYZ}}$ (Luther condition[23–25]), color correction techniques[4,21,26,27] must be applied *a posteriori* because systematic color errors will otherwise unavoidably arise. Because the Luther condition is seldom verified, we prefer to call $\mathbf{T_{RGB}}$ the "color matching pseudo-functions".

In this work, we show a strictly spectroradiometric method that provides an improved alternative to the pseudo-radiometric approach of the ISO 17321 standard.

Basic Optoelectronic Performance

If $n_\nu(\lambda)$ is the incident photon rate in the focal plane of a digital image capture device (scanner, camera) and $QE(\lambda)$ is the spectral quantum efficiency of the optoelectronic sensor, the total number of generated photoelectrons n_{pe} is:

$$\begin{aligned} n_{pe} &= \int_{360\,\mathrm{nm}}^{830\,\mathrm{nm}} n_{pe}(\lambda)\, d\lambda = \int_{360\,\mathrm{nm}}^{830\,\mathrm{nm}} n_\nu(\lambda) QE(\lambda)\, d\lambda \\ &\cong \sum_{360\,\mathrm{nm}}^{830\,\mathrm{nm}} n_\nu(\lambda) QE(\lambda)\, \Delta\lambda \end{aligned} \tag{5}$$

Therefore, the spectral quantum efficiency is the quantum version of the spectral sensitivity of the color reproduction system, and the above equation is the Rushton univariance principle applied to the physics of image capture.

In macroscopic ranges, it is advisable to change the photon irradiance $n_\nu(\lambda)$ for the spectral exposure $H(\lambda)$ (in joules), defined as follows.[28,29]

$$\begin{aligned} H(\lambda) &= \frac{hc}{\lambda} n_\nu(\lambda) \\ n_\nu(\lambda) &= \frac{\pi}{4} \frac{\lambda}{hc} \frac{L_e(\lambda) \cdot A_{\mathrm{SENSOR}} \cdot t}{N^2 \left(1 + m_{\mathrm{LENS}}\right)^2} \tau_{\mathrm{LENS}}(\lambda) \cdot T_{\mathrm{ATM}}(\lambda) \cdot \cos^4 \theta \end{aligned} \tag{6a}$$

where h and c are fundamental constants, L_e is the spectral radiance in W/sr·m² of the target or scene, A_{SENSOR} is the effective or irradiated sensor area, t is the photosite integration or exposure time of the shutter, N is the f-number or relative aperture of the zoom lens, m_{LENS} is the lateral magnification of the zoom lens, τ_{LENS} is the spectral transmittance of the zoom lens, T_{ATM} is the spectral transmittance of the atmosphere and θ is the angular position of the target with respect to the optical axis of the zoom lens.

In the majority of cases, it is correct to assume that τ_{LENS} and T_{ATM} are practically equal in the visible band of the electromagnetic spectrum, so we may simplify the equation above taking $\theta = 0$ (centered capture):

$$H(\lambda) = \alpha \frac{L_e(\lambda)}{N^2} t \quad ,$$
$$\text{with} \quad \alpha = \frac{\pi}{4} \frac{A_{SENSOR}}{(1 + m_{LENS})^2} \tag{6b}$$

From Eq. 6, the spectral exposure $H(\lambda)$ is directly proportional to the spectral radiance $L_e(\lambda)$ of the visual stimulus and the exposure time t and inversely proportional to the square of the f-number N of the zoom-lens. Nevertheless it is not certain, *a priori*, that all the possible combinations of the exposure series ($L_{e\lambda}$, N, t) that yield the same spectral exposure $H(\lambda)$ are going to generate the same digital response $DL(\lambda)$. This is known as *reciprocity failure*, which is not verified under some conditions in photochemical photography.[30,31] Until now, the verification of this radiometric law in digital photography has been little studied. In recent work,[32] we proved that the reciprocity law is completely verified by using monochromatic light and varying the f-number N or the exposure time t, or both simultaneously. These important results will be taken into account below in the development of this work.

In the final step of the optoelectronic transfer from generated photoelectrons n_{pe} to digital levels DL, an optoelectronic conversion constant K_λ (e^-/DL) may be used.[28,29] Hence, for each color-channel the relative digital spectral response NDL_λ is described by:

$$NDL_\lambda = H_\lambda \left[\frac{1}{\left(2^{bits} - 1\right)} \frac{\lambda}{hc} \frac{QE_\lambda}{K_\lambda} \right] \tag{7}$$

where H_λ and QE_λ are the dense versions of the spectral exposure and the spectral quantum efficiency respectively.

If we reformulate the above from the point of view of systems theory, in the sense that the response to an input may be written as *response = energy*sensitivity*. In Eq. 7 the spectral exposure plays the role of the energy input and the rest of the variables enclosed in brackets may be considered as the spectral sensitivity of the digital image capture system. Therefore, one direct method of spectral characterization is to find empirically the relation NDL_λ vs. H_λ, which we denote as *optoelectronic conversion spectral function* (OECSF).

Alternatively, two equivalent concepts may be derived from the general concept of spectral sensitivity[33]:

- *Spectral responsivity* $r(\lambda,H)$: the response to spectral stimuli with constant energy

$$r_{\lambda i} \equiv r_i(\lambda, H) = \frac{response(NDL_\lambda)}{constant\ energy(H)}, \; i = R,G,B\ channels \tag{8}$$

- *Action spectrum* $a(\lambda,NDL)$: the inverse of the energy of the spectral stimuli which give a constant response

$$a_{\lambda i} \equiv a_i(\lambda, NDL) = \frac{cons\tan t\ response(NDL)}{energy(H_\lambda)}, \; i = R,G,B\ channels \tag{9}$$

Because both concepts are going to be very important for the development of this work, we have considered it appropriate to analyze them further by comparing two kinds of image capture systems: the CIE-1931 XYZ Standard Observer, considered an ideal linear photosensor, and a real digital image capture device. In the first case, due to the strict linearity of the photosensor, the spectral responsitivity and the action spectrum for each color channel XYZ will not depend directly on the spectral exposure (or spectral radiance) nor on the response (spectral tristimulus value). The spectral profiles of these radiometric functions will then coincide directly with the color matching functions (CMF):

$$\begin{aligned} &r_{\lambda i} \equiv r_i(\lambda) \\ &a_{\lambda i} \equiv a_i(\lambda) \\ &r_{\lambda i} \equiv a_{\lambda i} \equiv CMF_{\lambda i} \quad , i = X,Y,Z\ channels \end{aligned} \tag{10}$$

If we now consider a real digital image capture device, we shall assume that, regardless of the linear range width, both radiometric functions are bidimensional and related directly to the optoelectronic conversion spectral function (OECSF):

$$\left.\begin{aligned} r_{\lambda i} \equiv r_i(\lambda, H) &= \frac{OECSF_i}{H} \\ a_{\lambda i} \equiv a_i(\lambda, NDL) &= \frac{NDL}{OECSF_i^{-1}} \end{aligned}\right\} \tag{11}$$

$$\text{with} \quad NDL_\lambda\ versus\ H_\lambda\ curve \equiv OECSF$$

Assuming that this radiometric formalism is correct, if we want to develop linear models to predict the response of digital image capture devices it is necessary to test the following linearity condition: the relative scaling of their complete (3-D) spectral responsivities (action spectra) should be constant when the spectral exposure (normalized digital level) varies. Only if this assumption holds may we successfully obtain the spectral characterization of any digital camera and transform it into an absolute tele-colorimeter using a basic transformation between the RGB camera space and the CIE-1931 XYZ space.

This work shows a new method of obtaining the representative color matching pseudo-functions $\mathbf{T}_{RGB}$ associated with the real spectral responsivities of any digital image capture system, which allows us to test the linear performance of these color devices and use them as pseudo-colorimetric instruments. This method was performed on real spectroradiometric data and consisted of the following stages:

a) Spectral characterization: measurement and characterization of the optoelectronic conversion spectral functions (OECSF) and the complete spectral responsivities $r_i(\lambda,H)$, or equivalently, the action spectra $a_i(\lambda,NDL)$.
b) Colorimetric characterization: calculation of the color matching pseudo-functions $\mathbf{T}_{RGB}$ from the complete spectral sensitivities. This algorithm will consider the absolute scaling between the spectral sensitivities of the three color channels and the real white balance configured initially following manufacturer specifications (camera menu), and which is never adjusted in a colorimetric sense.

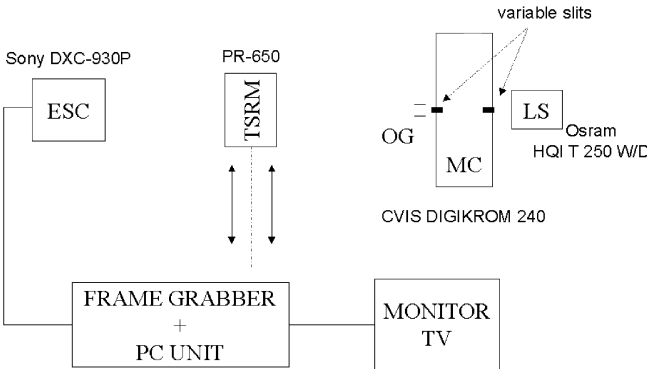

Figure 1. Experimental set-up.

c) A real illumination-scene test to predict the RGB digital levels applying a single camera pseudo-tristimulus model.

Spectral Characterization

Set-up and Procedure

Figure 1 shows the experimental set-up. Our digital image capture device (electronic still camera, ESC) consisted of a Sony DXC-930P 3CCD-RGB video camera connected to a Matrox MVP-AT 850 frame grabber inserted into a PC unit. Target radiance was varied using the entrance/exit slits of a CVIS Laser Digikröm monochromator (MC) with constant spectral resolution, connected to an Osram HQI T 250W/Daylight vapor fluorescent lamp (LS). There were no additional lamps or residual lights inside the laboratory during the capture of the monochromatic target (opal glass, OG). The monochromator-target distance was adjusted to get a spatially-homogeneous radiance field into the target.

Among the fixed initial conditions, which might alter the color output data, we set the white balance to 5600 K in manual menu-mode (offset value) and configured the gain and the offset of the analog–digital converter (ADC) to ensure minimal influence on color output data, according to the manufacturer's specifications. With these initial parameters, we ensured that the RGB data were raw, without unknown internal color matrixing. The target radiance $L_{e\lambda}$ was measured by a Photo Research PR-650 tele-spectroradiometer (TSRM) for the 380–780 nm wavelength range in 10 nm steps, maintaining the photosite integration time at t = 20 ms (offset value) with some selected f-numbers N. This procedure is possible because we had previously proven that the system verifies the reciprocity. The spectral exposure H_λ averaged in the exposure series ($L_{e\lambda}$, N, t = 20 ms) for each monochromatic image was given by:

$$H_\lambda = 514.9823\, e-9\, \frac{L_{e\lambda}}{N^2}\, t \tag{12}$$

Dark current/frame subtraction was applied to each monochromatic image and the normalized digital level *NDL* was obtained by averaging eight statistical windows larger than 64 × 64 pixels.

Results

The optoelectronic conversion spectral functions (OECSFs), that is, the NDL_λ versus H_λ curves for each RGB channel, were fitted mathematically by sigmoid functions, defined by four parameters as follows:

$$NDL_{\lambda i} = a_{\lambda i} + \frac{b_{\lambda i}}{1+\exp\left(-\dfrac{H_\lambda - c_{\lambda i}}{d_{\lambda i}}\right)} \tag{13}$$

For the CIE-1931 XYZ standard observer, the equivalent *OECSFs* are essentially the same as in the XYZ channels:

$$\begin{aligned} X_\lambda &= \left(683\,\bar{x}_\lambda\,\Delta\lambda\right) L_{e\lambda} \\ Y_\lambda &= \left(683\,\bar{y}_\lambda\,\Delta\lambda\right) L_{e\lambda} \\ Z_\lambda &= \left(683\,\bar{z}_\lambda\,\Delta\lambda\right) L_{e\lambda} \end{aligned} \tag{14}$$

According to these equations, the CIE-1931 XYZ standard observer is considered as a linear color image sensor. However, any digital still camera is strictly speaking a non-linear color image sensor because its *OECSFs* are non-linear functions. For example, Fig. 2 shows the experimental results for λ = 570 nm in the R and G channels. The B channel was not sensitive at this wavelength, unlike other digital still cameras. In the CIE-1931 XYZ case (Fig. 2, bottom), the three XYZ channels respond to this wavelength and the three *OECSFs* are linear although they are represented in logarithmic axes.

From these experimental and modeling data, the spectral responsivities $r_R(\lambda,H)$, $r_G(\lambda,H)$, $r_B(\lambda,H)$ and the action spectra $a_R(\lambda,NDL)$, $a_G(\lambda,NDL)$, $a_B(\lambda,NDL)$ are obtained by:

$$\begin{aligned} responsivity &= \frac{response}{constant\ energy} \\ r_i(\lambda,H) &= \frac{a_{\lambda i} + \dfrac{b_{\lambda i}}{1+\exp\left(-\dfrac{H - c_{\lambda i}}{d_{\lambda i}}\right)}}{H} \end{aligned} \tag{15}$$

$$\begin{aligned} action\ spectrum &= \frac{constant\ response}{energy} \\ a_i(\lambda,NDL) &= \frac{NDL}{c_{\lambda i} - d_{\lambda i}\ln\left(\dfrac{b_{\lambda i}}{NDL - a_{\lambda i}} - 1\right)} \end{aligned} \tag{16}$$

Figures 3 (top) and 4 (top) show the spectral responsivities and the action spectra of our digital image capture system for λ = 570 nm, obtained according to Eqs. 15 and 16. Figures 3 (bottom) and 4 (bottom) show the same functions for the CIE-1931 XYZ derived from Eq. 14. In this case the spectral responsivities and the action spectrum would be constant versus radiance (energy) and tristimulus value (response) and are equal to for the X channel, for the Y channel and for the Z channel. For our digital image capture system the behavior is clearly non-linear, as can be seen in Figs. 3 (top) and 4 (top). The sudden rise in the responsivity or in the action spectrum indicates that the spectral expo-

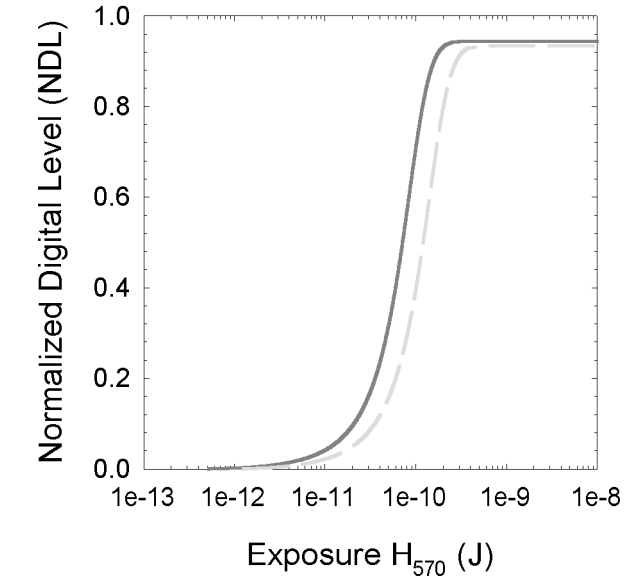

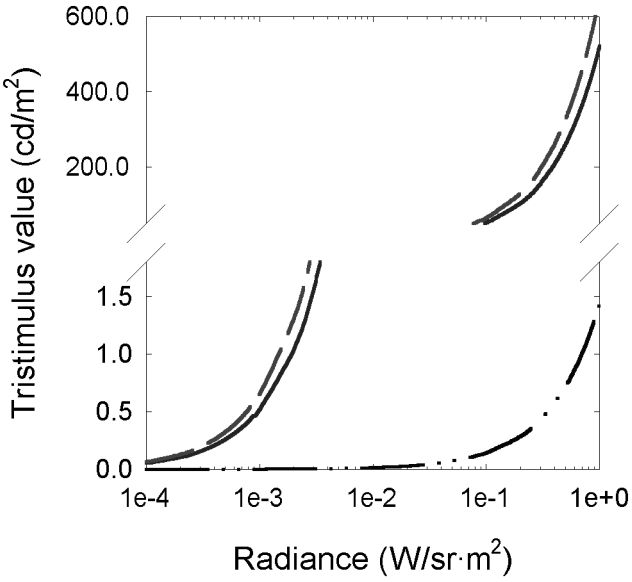

Figure 2. Top: OECSFs measured with λ = 570 nm, corresponding to the R and G channel of a Sony DXC-930P video camera plus a Matrox MVP-AT 850 frame grabber. Bottom: OECSFs calculated for CIE-1931 XYZ Standard Observer with the same wavelength. (Solid line: R/X channel; dashed line: G/Y channel; dash–dot–dotted line: B/Z channel.)

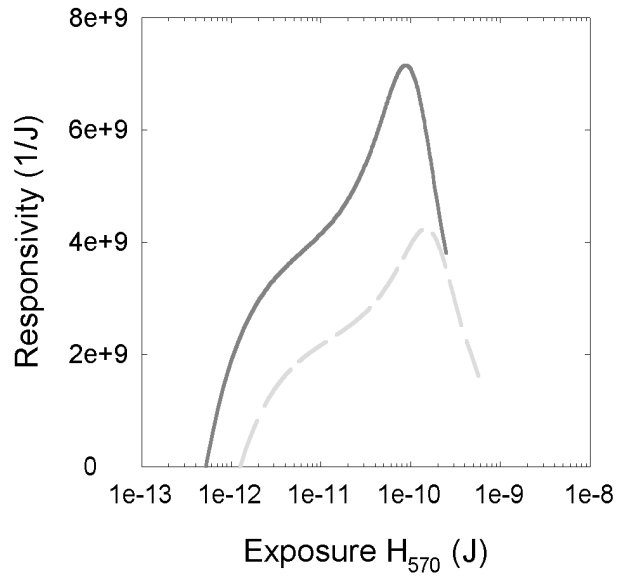

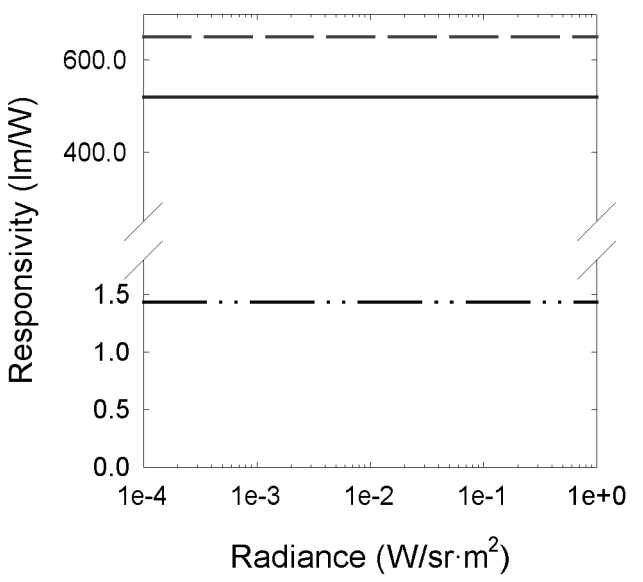

Figure 3. Top: spectral responsivities of the R and G channels of a Sony DXC-930P video camera plus a Matrox AT-850 frame grabber measured with λ = 570 nm. Bottom: spectral responsivities for CIE-1931 XYZ Standard Observer with the same wavelength. (Solid line: R/X channel; dashed line: G/Y channel; dash–dot–dotted line: B/Z channel.)

sure (incident photon rate) surpasses the optoelectronic threshold level (dark current/frame photocurrent). The sudden drop in the responsivity (action spectrum) when the digital value approaches its maximum level indicates the saturation of the full optoelectronic wells in both channels. Both effects are common to many real biological or artificial photosensors,[34] although they do not appear in the ideal linear color sensor CIE-1931 XYZ. In the middle range, the responsivity (action spectrum) varies smoothly versus spectral exposure (normalized digital level), but never linearly like a true linear image sensor.

Figures 3 and 4 are the two-dimensional profiles of $r_i(\lambda,H)$ and $a_i(\lambda,NDL)$ 3-D functions (**Color Plates 7 and 8, pp. 56–57**). The important question is whether the relative scaling of the spectral responsivity (action spectrum) remains constant when we select spectral profiles with different constant exposures (or equivalently, normalized digital levels) even if the absolute scaling changes. As shown in Fig. 5 for the three color channels, this assumption holds despite slight experimental and modeling deviations. The absolute scaling of the respective action spectra changes with normalized digital level (**Color Plate 8, p. 57**),

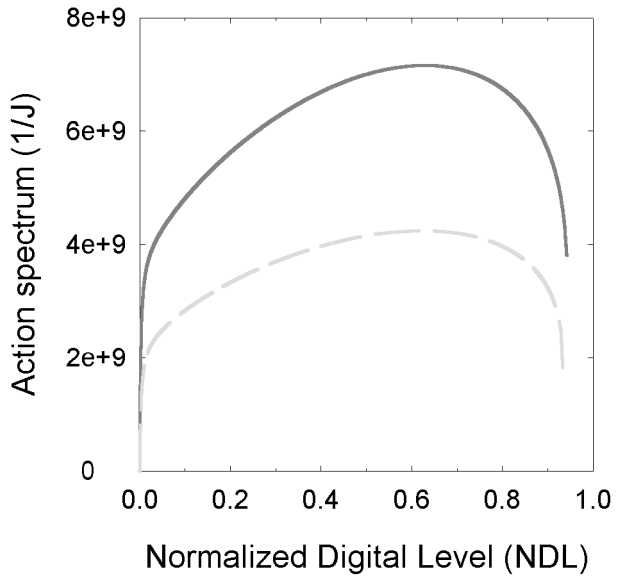

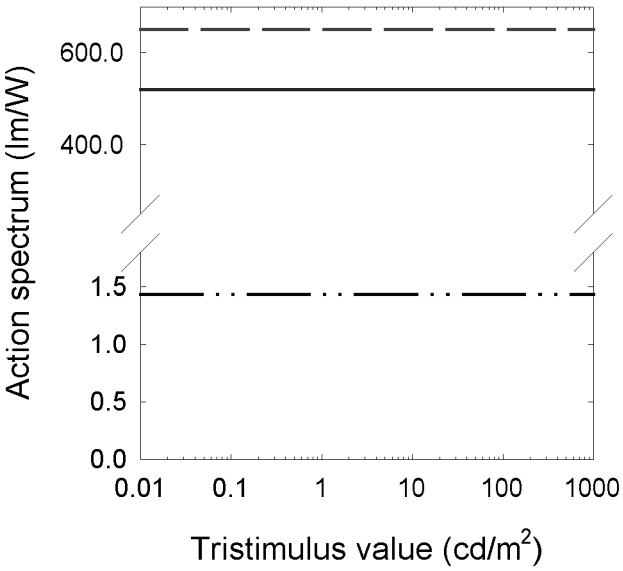

Figure 4. Top: action spectra of the R and G channels of a Sony DXC-930P video camera plus a Matrox AT-850 frame grabber measured with $\lambda = 570$ nm. Bottom: action spectra for CIE-1931 XYZ Standard Observer with the same wavelength. (Solid line: R/X channel; dashed line: G/Y channel; dash–dot–dotted line: B/Z channel.)

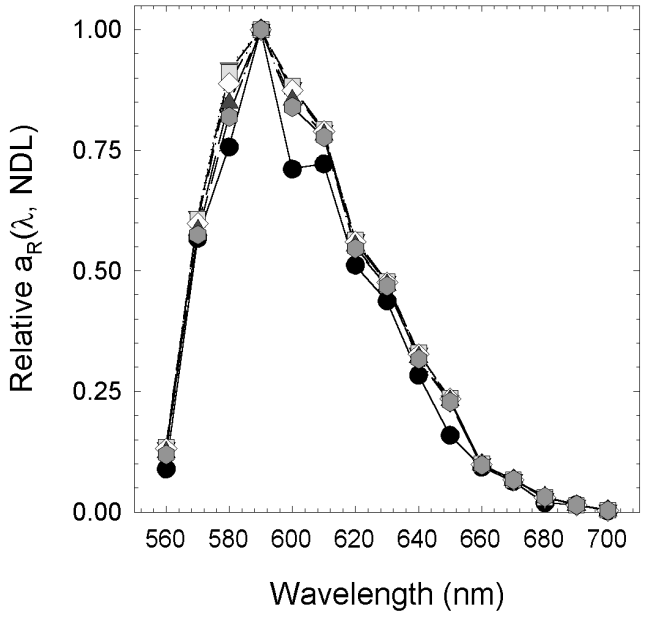

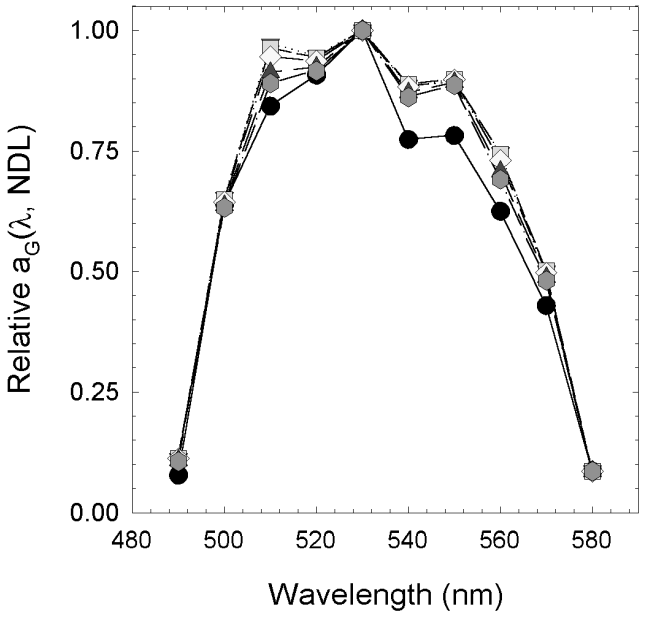

Figure 5. Relative scaling of the action spectra (spectral responsivities) of the RGB channels of our digital image capture device. The solid symbols correspond to the following normalized digital levels: 1/255 (threshold, lower solid-line), 10/255, 0.1, 0.2, 0.5 and 0.8. (Top: R channel; center: G channel; bottom: B channel.)

although the relative scaling remains approximately the same (Fig. 5).

Colorimetric Characterization

We have proved above that if we select different normalized digital levels in the action spectrum of each color channel, the absolute scaling is different in each spectral profile (**Color Plate 7, p. 56**), but the relative scaling is approximately the same, as shown for the RGB channels (Fig. 5). This means that we can define the relative spectral sensitivity as the average of some spectral profiles (Fig. 6). This last graphical result is the typical technical report provided by most manufacturers to serve as the spectral characterization of their product, but this kind of information hides the joint relative scaling of the color channels. For instance, in the CIE-1931 XYZ case, it is not usual to plot the color matching functions $\mathbf{T}_{XYZ}$ in relative format (between 0 and 1), but the joint relative scaling is 1.0622 : 1 : 1.7721.

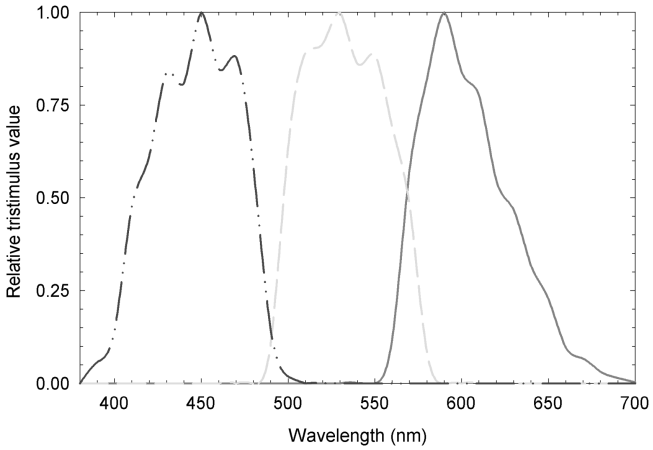

Figure 6. Relative spectral sensitivities of a Sony DXC-930P video camera plus a Matrox AT-850 frame grabber. (Solid line: R channel; dashed line: G channel; dash–dot–dotted line: B channel.)

Hence, the next problem is to rescale the maximum levels in the RGB action spectra because their absolute scales are not identical. Moreover, this question cannot be solved independently of the calculation of the colorimetric or real white balance of our digital image capture device: although the white balance provided by the manufacturer was 5600 K, this does not mean that the true white balance is 1:1:1. Therefore, this stage of the general algorithm is centered on obtaining the color matching pseudo-functions $\mathbf{T}_{\mathbf{RGB}}$, taking into account the joint relative scaling and the colorimetric white balance of the relative spectral sensitivities. With this in mind, we present this section in several stages that, algorithmically, are connected sequentially.

Proposed Camera Formula

From this radiometric formalism and taking into account Eq. 5, a new digital pseudo-tristimulus value formula is proposed:

$$\begin{aligned} DL_i &= \left(2^{bits}-1\right)\sum_{380\,nm}^{780\,nm} NDL_{\lambda i}\,\Delta\lambda \\ &= \left(2^{bits}-1\right)\sum_{380\,nm}^{780\,nm} H_\lambda \cdot r_i(\lambda,H)\,\Delta\lambda \end{aligned} \tag{17}$$

Relative Scaling

In our experimental data, the maximum responsivity-peaks were λ_R = 590 nm, λ_G = 530 nm and λ_B = 450 nm. From Eq. 17, we obtained the joint relative scaling of the three spectral responsivities $r_{590R} : r_{530G} : r_{450B} = 1 : 0.6907 : 0.8753$. Let us define $p_R = 1$, $p_G = 0.6907$ and $p_B = 0.8753$. (For the CIE-1931 XYZ case, λ_R = 600 nm, λ_G = 555 nm, λ_B = 450 nm and 1.0622 : 1 : 1.7721.) Therefore, the relative spectral responsivities (action spectra) are defined as:

$$\begin{aligned} &\mathbf{r}'_R(\lambda) = \frac{p_R}{r_{\lambda_R}}\,\mathbf{r}_R(\lambda); \quad \mathbf{r}'_G(\lambda) = \frac{p_G}{r_{\lambda_G}}\,\mathbf{r}_G(\lambda); \\ &\mathbf{r}'_B(\lambda) = \frac{p_B}{r_{\lambda_B}}\,\mathbf{r}_B(\lambda) \end{aligned} \tag{18}$$

where $r_{\lambda_R}, r_{\lambda_G}$ and r_{λ_B} are the absolute maximum responsivity-peaks.

White Balance Test

The white balance algorithm consists of performing another scaling on the spectral functions in Eq. 18 depending on the resulting chromatic response to an equal energy stimulus **E**, regardless of the absolute radiant level. To understand this process, it is best to analyze the ideal linear color image sensor: CIE-1931 XYZ Standard Observer. With $\Delta\lambda$ = 5 nm, we obtain[33]

$$\bar{\mathbf{x}}^{\mathrm{t}} \cdot \mathbf{E}\ , \bar{\mathbf{y}}^{\mathrm{t}} \cdot \mathbf{E}\ , \bar{\mathbf{z}}^{\mathrm{t}} \cdot \mathbf{E}\ = 21.3714\,;$$

this means a balance of 1:1:1, that is, the ideal linear color image sensor is balanced to the equal energy stimulus (adapted white according to ISO 17321). However, although the electronic white balance was apparently configured to 1:1:1 according to the manufacturer, we are not sure whether this white balance is correct from the colorimetric point of view, regardless of the white adopted. Therefore, we are obliged to test it and compensate for it if it is not correct.

Because the real digital image capture devices are not strictly linear, we must test the equal energy white balance for each absolute exposure level. This is done using Eq. 17, by maintaining H_λ constant with all the spectroradiometric data (the values a, b, c, d of the OECSFs). Figure 7 (top) shows that if the white balance were 1:1:1 the three curves would overlap, but instead the blue channel is always the most sensitive of the three channels, and therefore the first to saturate. If, on the other hand, we plot jointly the three equal energy responses, we see that there are linear relations between them (Fig. 7, bottom). If we choose the blue channel as a reference, instead of the red channel which is chosen in the joint relative scaling, the inverses of the slopes of the straight lines NDL_R versus NDL_B and NDL_G versus NDL_B are, respectively, 0.8642 and 0.6839. If we call these slopes bal_R, bal_G, bal_B (= 1), the resulting true white balance is $bal_R : bal_G : bal_B$ = 0.8642 : 0.6839 : 1, and not 1:1:1 although the electronic white balance was initially fixed at 5600 K.

Calculation of the Color Matching Pseudo-Functions

The conversion of the relative RGB spectral sensitivities to the color matching pseudo-functions $\mathbf{T}_{\mathbf{RGB}}$ (41 rows by 3 columns) consisted finally of verifying the equal energy white balance:

$$\begin{aligned} &\bar{\mathbf{r}} \equiv \alpha_R\,\mathbf{r}'_R = \left(bal_R\,\frac{\mathbf{r}'^{\,\mathrm{t}}_B \cdot \mathbf{E}}{\mathbf{r}'^{\,\mathrm{t}}_R \cdot \mathbf{E}}\right)\mathbf{r}'_R \\ &\bar{\mathbf{g}} \equiv \alpha_G\,\mathbf{r}'_G = \left(bal_G\,\frac{\mathbf{r}'^{\,\mathrm{t}}_B \cdot \mathbf{E}}{\mathbf{r}'^{\,\mathrm{t}}_G \cdot \mathbf{E}}\right)\mathbf{r}'_G, \\ &\bar{\mathbf{b}} \equiv \alpha_B\,\mathbf{r}'_B = \left(bal_B\right)\,\mathbf{r}'_B \\ &\text{in order to } \mathbf{T}_{\mathbf{RGB}}{}^{\mathrm{t}} \cdot \mathbf{E} \propto \begin{bmatrix} bal_R \\ bal_G \\ bal_B \end{bmatrix} \end{aligned} \tag{19}$$

Finally, we can plot jointly (Fig. 8) at the same level the spectral sensitivities (color matching functions) of the ideal linear color image sensor CIE-1931 XYZ and our real digital image capture device. Even so, it is nec-

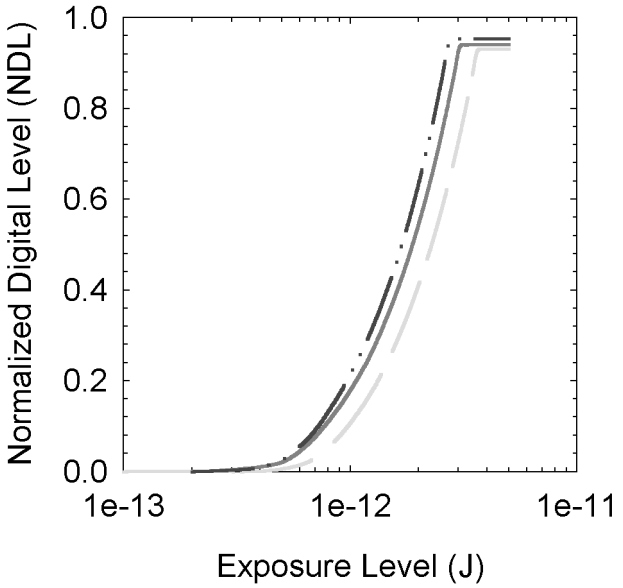

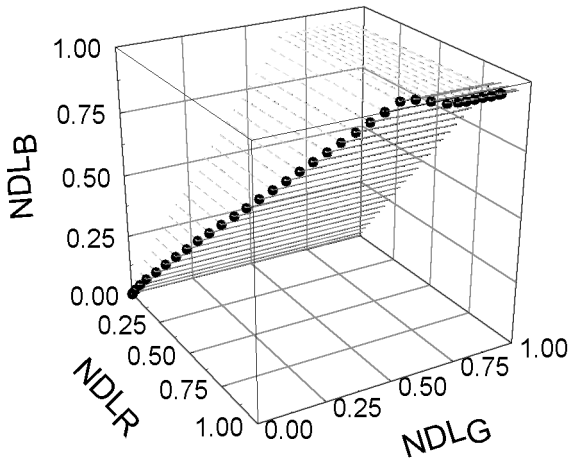

Figure 7. Colorimetric white balance test for our digital image capture device. Above: color responses to equal energy stimulus with different absolute exposure levels (Solid line: R channel; dashed line: G channel; dash–dot–dotted line: B channel). Bottom: the inverses of the slopes of the projected lines in R–B and G–B planes are 0.8642 and 0.6839 respectively.

essary to find the true scale of the blue channel, and of the rest, because we took $bal_B = 1$. However, with the procedure developed so far we cannot obtain this value. This is a task for the color correction techniques.

Real Illumination-Scene Test

The purpose of this section is to test a single camera model that recovers the RGB digital levels of the real captures of a scene under different illumination conditions. Although the algorithm employed to obtain the color matching functions was strictly spectroradiometric, unlike the ISO 17321 algorithm, we may use the color matching pseudo-functions, $\mathbf{T}_{\mathbf{RGB}}$, in the camera model because we may assume the camera to be linear and therefore Grassmann's laws (additivity and proportionality) will hold.

The real illumination-scene test was a Macbeth Color Checker inside a non-standard light box. A Photo Research PR-650 tele-spectraradiometer and a Halon reference white were used to measure the spectral radiances

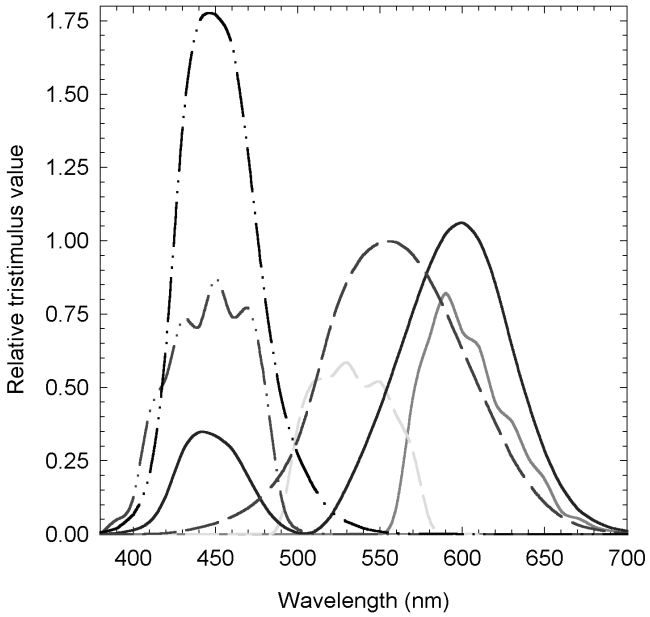

Figure 8. Color matching pseudo-functions of the Sony DXC-930P video camera plus a Matrox AT-850 frame grabber joint to the Standard Observer CIE-1931 XYZ. (Solid line: R or X channel; dashed line: G or Y channel; dash–dot–dotted line: B or Z channel.)

$L_{e\lambda}$ of all the chart patches under three different light sources: INC, halogen lamp; HWL, metal halide lamp; and DAY, daylight fluorescent lamp (**Color Plates 9–11, p. 58**). The camera and frame grabber conditions were the same as used in the above sections, that is, the white balance was fixed by control menu at 5600 K.

The test consisted of verifying whether the real RGB digital levels could be recovered by imposing a single camera model using the calculated color matching pseudo-functions $\mathbf{T}_{\mathbf{RGB}}$. If $\mathbf{t}_{\mathbf{RGB}}$ are the measured RGB digital levels without the dark current/frame noise, the recovered RGB digital levels $\mathbf{t'}_{\mathbf{RGB}}$ can be written as follows:

$$\mathbf{t}'_{\mathbf{RGB}} = \begin{bmatrix} R \\ G \\ B \end{bmatrix}$$

$$= \left(2^{bits} - 1\right)\Delta\lambda \begin{bmatrix} k_R & 0 & 0 \\ 0 & k_G & 0 \\ 0 & 0 & k_B \end{bmatrix} \mathbf{T}_{\mathbf{RGB}}{}^{\mathrm{t}} \cdot \mathbf{c}, \text{ with } \mathbf{c} = \mathrm{diag}(\mathbf{L}) \cdot \rho$$

$$\Rightarrow \begin{bmatrix} DL'_R \\ DL'_G \\ DL'_B \end{bmatrix}$$

$$= \begin{cases} noise_{i=R,G,B}, \text{ if } R,G,B \le 0 \\ \mathbf{t}'_{\mathbf{RGB}} + \begin{bmatrix} noise_R \\ noise_G \\ noise_B \end{bmatrix}, \text{if } 0 < R,G,B < \left(2^{bits} - 1\right) - noise_{i=R,G,B} \\ \left(2^{bits} - 1\right), \text{if } R,G,B \ge \left(2^{bits} - 1\right) - noise_{i=R,G,B} \end{cases} \quad (20)$$

where $bits = 8$, $\Delta\lambda = 10$ nm, $\mathrm{diag}(\mathbf{L})$ is the diagonal format of the light source vector and ρ is the spectral reflectance vector. The matrix $\mathbf{K}$ must be diagonal, without

TABLE II. Numerical Results of the Predicted Data Under INC Lamp: k_R = 11.6, k_G = 13.0, k_B = 12.1.

	Mean	Max	Min
log (absolute RGB error)	0.93	1.23	0.60
log (relative RGB error)	1.07	1.81	0.33
ΔE (CIE-L*a*b*)	4.65	14.12	1.73

TABLE III. Numerical Results of the Predicted Data Under HWL Lamp: k_R = 4.1, k_G = 6.3, k_B = 5.4.

	Mean	Max	Min
log (absolute RGB error)	1.43	1.97	0.82
log (relative RGB error)	1.24	1.79	0.33
ΔE (CIE-L*a*b*)	13.32	37.02	3.64

TABLE IV. Numerical Results of the Predicted Data Under DAY Lamp: k_R = 5.9, k_G = 5.5, k_B = 5.8.

	Mean	Max	Min
log (absolute RGB error)	1.12	1.34	0.94
log (relative RGB error)	1.13	1.84	0.79
ΔE (CIE-L*a*b*)	9.78	16.79	3.98

crossing elements, in order to verify the Grassmann laws.

The dark current/frame noises are respectively 15.2, 17.7 and 11.9. The *f*-number N was set to 4 for the INC lamp and 5.6 for the HWL and DAY lamps, but the photosite integration time t was always fixed to 20 ms (offset value).

Because the measured RGB digital levels initially had noise, we preferred to work directly with these RGB data, $[DL_R , DL_G , DL_B]^t$, and compare them with the recovered RGB data $[DL'_R , DL'_G , DL'_B]^t$. Tables II–IV show the numerical results in absolute root-mean-square or RMS RGB error, relative RMS RGB error and average ΔE in CIE-L*a*b* color space, assuming that the RGB digital levels are displayed on an sRGB monitor. These results are also shown graphically in Fig. 9. The experimental RGB data due to pixel clipping (in both extremes) are included because they are also recovered.

These results have proved that by using a unique set of color matching pseudo-functions with a unique colorimetric white balance (usually different from the electronic white balance) the RGB data are recovered very well, whatever the chromaticity of the light source. As well as imposing a joint relative scaling and the colorimetric white balance in the relative spectral sensitivities, the single camera model predicts the pixel clipping quite well in both extremes. Moreover, these results show again, as in similar experiments, the difficulty of recovering RGB data using spectrally non-homogeneous light sources: the INC results are the best and the HWL results are the worst. An additional result is that the diagonal coefficients have the same ratio as the *f*-numbers of the captures: for the HWL and DAY lamps, N was 5.6 and the coefficients are approximately 6. For the INC lamp, the coefficients fluctuate around 12 because the *f*-number N was 4 (twice as large as the others).

Because the diagonal matrix $\mathbf{K}$ is dependent on the *f*-number N of the digital image capture device and possibly of the spectral sampling $\Delta\lambda$ (= 10 nm) that we performed, we believe that more work is necessary on this subject in order to obtain a complete camera model which covers all the realistic illumination-scene environments (spatially non-uniform illumination field, variable chromaticity and large dynamic range of luminance levels) in order to transform a spectracolorimetrically

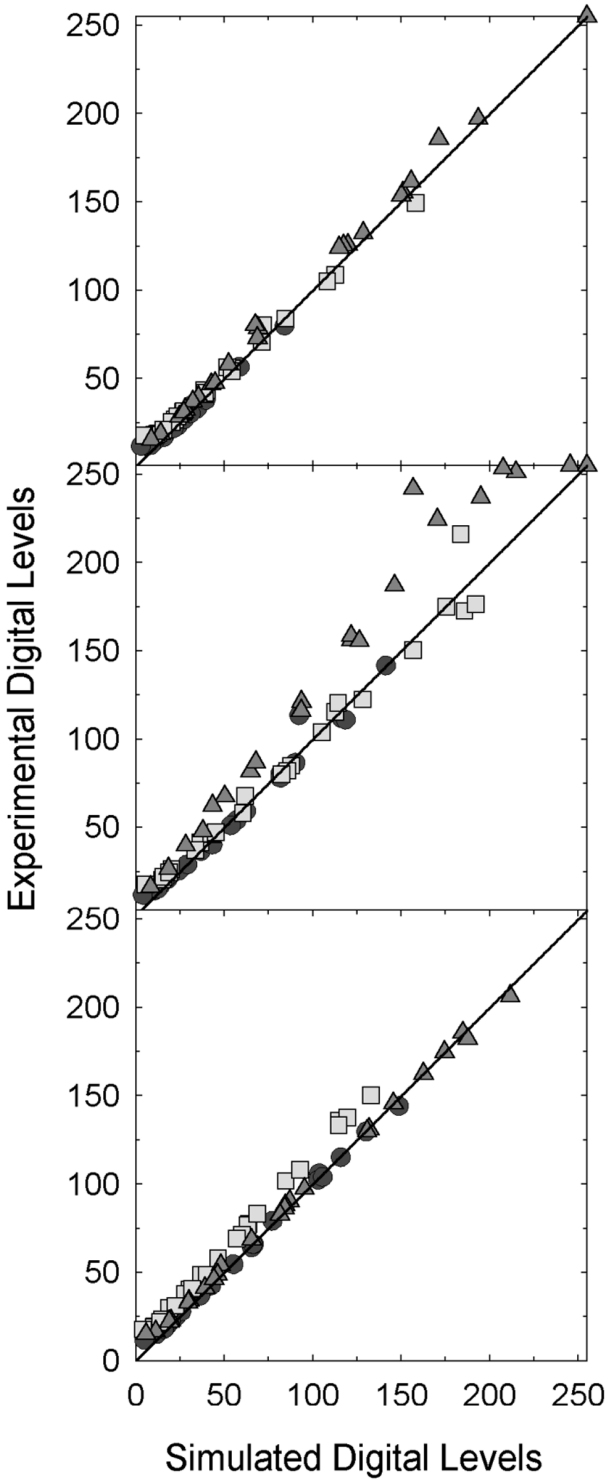

Figure 9. Prediction of the RGB digital levels of the Macbeth Color-Checker Chart under three light sources: top, INC lamp; center: HWL lamp; bottom: DAY lamp. The *x*–*y* axes indicate the simulated and experimental data respectively (Circles: B channel; squares: G channel; triangles: R channel).

characterized digital camera into an absolute telecolorimeter.

Conclusions

We have presented an experimental and general spectral characterization for any digital image capture device (scanner, camera) using the equivalent terms of spectral responsivity and action spectrum. We have also proved that any digital image capture device is strictly speaking a non-linear color image sensor because its spectral sensitivities are not constant versus the spectral exposure and normalized digital level. In the CIE-1931 XYZ observer, which is considered to be a linear system, spectral sensitivities remain constant with changing exposure or response. The relative spectral sensitivities of the digital image capture device, however, are independent of spectral exposure or normalized digital level, and this circumstance allows us to work with these color devices as if they were linear.

From the absolute spectral sensitivities (responsivity or action spectrum mode), the absolute scaling of the three color channels and the colorimetric or real white balance, and the color matching pseudo-functions have been obtained for a typical digital still camera. The resulting pseudo-color matching functions have been used to predict the RGB digital levels of a real illumination-scene test using a single camera model. However, this model is dependent on the relative aperture (*f*-number) of the zoom lens, so more research on this subject is needed to extend this performance to any dynamic luminance range. With the final purpose of using any digital camera as a telecolorimeter, in advanced research which concerns other work, we have converted our RGB camera data to absolute CIE-XYZs including a new algorithm of luminous adaptation based on the variation of the relative aperture of the zoom lens.

Acknowledgments. This research was supported by the Comisión Interministerial de Ciencia y Tecnología (CICYT) (Spain) under grants TAP96-0887 and TAP99-0856.

References

1. R. W. G. Hunt, *The Reproduction of Colour*, 5th ed., Fountain Press, Kingston-upon-Thames, 1995.
2. G. G. Field, *Color and Its Reproduction*, 2nd ed., GATF Press, Pittsburgh, PA, 1999.
3. R. M. Adams II and J. B. Weisberg, *The GATF Practical Guide to Color Management*, GATF Press, Pittsburgh, 1998.
4. H. R. Kang, *Color technology for electronic imaging devices*, SPIE Press, Bellingham, WA, 1997.
5. G. Sharma and H.J. Trussell, Digital color imaging, *IEEE Trans. Image Process* **6**, 901 (1997).
6. J. B. Cohen, Color and color mixture: Scalar and Vector fundamentals, *Color Res. Appl.* **13**, 5 (1988).
7. H. J. Trussell, Application of Set Theoretic Methods to Color Systems, *Color Res. Appl.* **16**, 31 (1991).
8. G. Sharma, H. J. Trussell and M. J. Vhrel, Optimal nonnegative color scanning filters, *IEEE Trans. Image Process* **7**, 129 (1998).
9. The International Organization for Standardization (ISO), ISO/TC42 (Photography), WG18 (Electronic Still Picture Imaging), ISO/TC130 (Graphic Technology), WG3 (Prepress Digital Data Exchange), *WD 4 of ISO 17321: Graphic Technology and Photography – Color characterization of digital still cameras (DSCs) using color targets and spectral illumination*, Geneva (1999).
10. The International Organization for Standardization (ISO), ISO/TC42 (Photography), WG18 (Electronic Still Picture Imaging), *DIS - ISO 14524: Photography – Electronic still picture cameras – Methods for measuring opto-electronic conversion functions (OECFs)*, Geneva (1999).
11. European Broadcasting Union (EBU), *3237-E: Methods of measurement of the colorimetric fidelity of television cameras*, 2nd ed., Brussels, Belgium (1989).
12. The International Electrotechnical Commission (IEC), Technical Committee no. 100: Audio, Video and Multimedia Systems and Equipment, Project Team 61966, Color Measurement and Management in Multimedia Systems and Equipment – Part 9: Digital cameras, *100/PT61966(PL)84, IEC/3WD 61966-9: Color Measurement and Management in Multimedia Systems and Equipment – Part 9: Digital cameras*, Vienna (1999).
13. M. J. Vhrel and H. J. Trussell, Color Device Calibration: A Mathematical Formulation, *IEEE Trans. Image Process* **8**, 1796 (1999).
14. W. K. Pratt and C. E. Mancill, Spectral estimation techniques for the spectral calibration of a color image scanner, *Appl. Opt.* **15**, 73 (1976).
15. P. Vora and H. J. Trussell, Mathematical methods for the analysis of color scanning filters, *IEEE Trans. Image Process* **6**, 312 (1997).
16. G. D. Finlayson, S. Hordley and P. M. Hubel, Recovering Device Sensitivities with Quadratic Programming, *Proc. IS&T/SID 6th Color Imaging Conference*, IS&T, Springfield, VA, 1998, pp. 90–95.
17. J. Y. Hardeberg, F. Schmitt, H. Brettel, J–P. Crettez, and H. Maître, Multispectral Image Acquisition and Simulation of Illuminant Changes, *Colour Imaging: Vision and Technology*, L.W. MacDonald and R. Luo, Eds., John Wiley and Sons, New York, 1999.
18. G–W. Chang and Y–C. Chen, Colorimetric modeling for vision systems, *J. Electronic Imaging* **9**, 432 (2000).
19. G. Sharma and H. J. Trussell, Set theoretic estimation in color scanner characterization, *J. Electronic Imaging* **5**, 479 (1996).
20. G. Sharma, Targetless Scanner Color Calibration, *J. Imaging Sci. Technol.* **44**, 301 (2000).
21. G. D. Finlayson and M. S. Drew, Constrained least-squares regression in colour spaces, *J. Electronic Imaging* **6**, 484 (1997).
22. G. Sharma and H. J. Trussell, Figures of merit for color scanners. *IEEE Trans. Image Process.* **6**, 990 (1997).
23. R. Luther, Aus Dem Gebiet der Farbreizmetrik, *Z. Tech. Phys.* **8**, 540 (1927).
24. H. E. Ives, The transformation of color-mixture equations from one system to another, *J. Franklin Inst.* **16**, 673 (1915).
25. B. K. P. Horn, Exact reproduction of colored images, *Comput. Vis. Graph. Image Process* **26**, 135 (1984).
26. V. C. Cardei and B. Funt, Color Correcting Uncalibrated Digital Images, *J. Imaging Sci. Technol.* **44**, 288 (2000).
27. G. D. Finlayson and P. M. Morovic, Metamer Constrained Color Correction, *J. Imaging Sci. Technol.* **44**, 295 (2000).
28. G. C. Holst, *CCD Arrays, cameras and displays*, 2nd ed., SPIE Press, Bellingham, WA, 1998.
29. J. R. Janesick, *Charge-Coupled Devices*, SPIE Press, Bellingham, WA, 2000.
30. J. F. Hamilton, Reciprocity failure and the intermittency effect, in *The Theory of the Photographic Process*, 4th ed., T.H. James, Ed., MacMillan, New York, 1977, p. 133.
31. B. H. Carroll, G. C. Higgins and T. H. James, *Introduction to photographic theory. The silver halide process*, John Wiley & Sons, New York, 1980, p. 13.
32. F. Martínez–Verdú, J. Pujol and P. Capilla, Testing the Reciprocity Law in Digital Photography, *J. Electronic Imaging*, in press.
33. G. Wyszecki and W. S. Stiles, *Color Science: Concepts and Methods, Quantitative Data and Formulae*, 2nd ed., John Wiley and Sons, New York, 1982.
34. J. C. Dainty and R. Shaw, *Image Science: principles, analysis and evaluation of photographic-type imaging processes*, Academic Press, London, 1974.

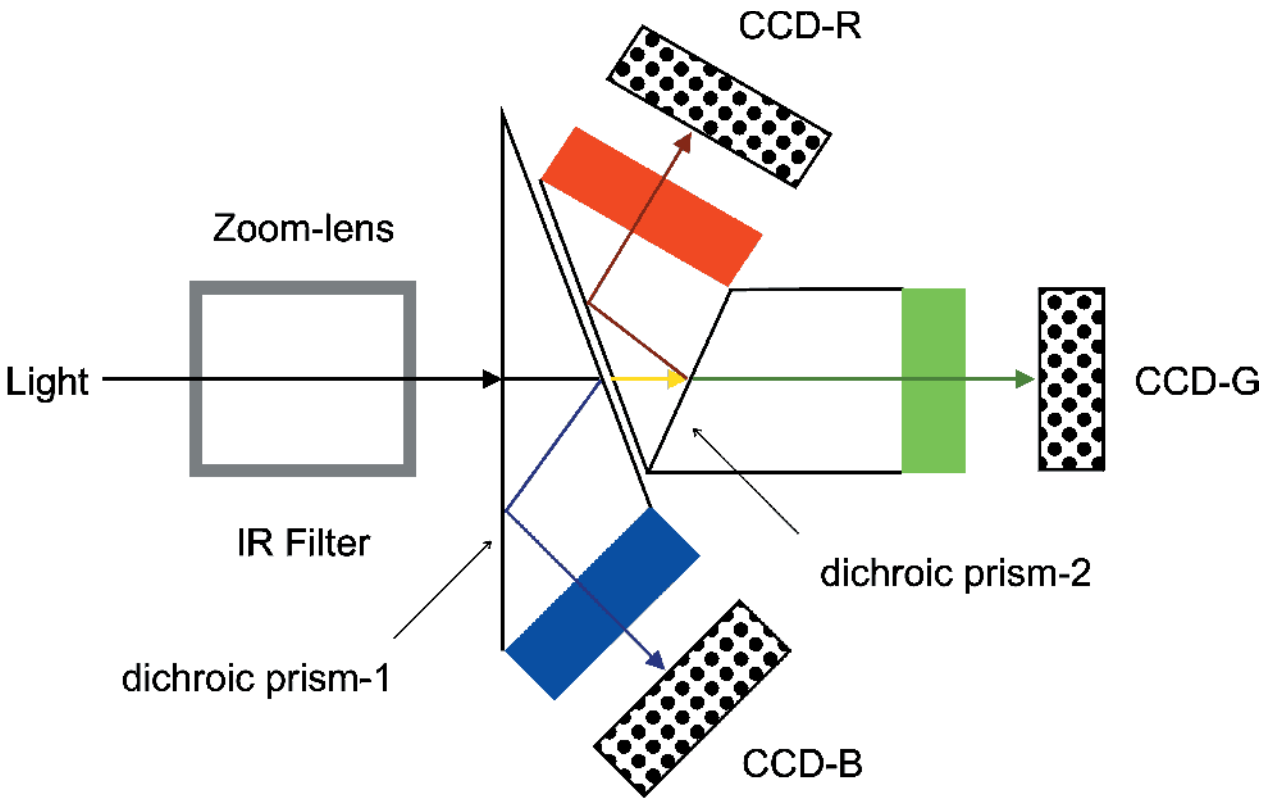

Color Plate 6. Diagram of the optical design of a 3-CCD camera. (Martínez-Verdú, et al., pp. 15–25)

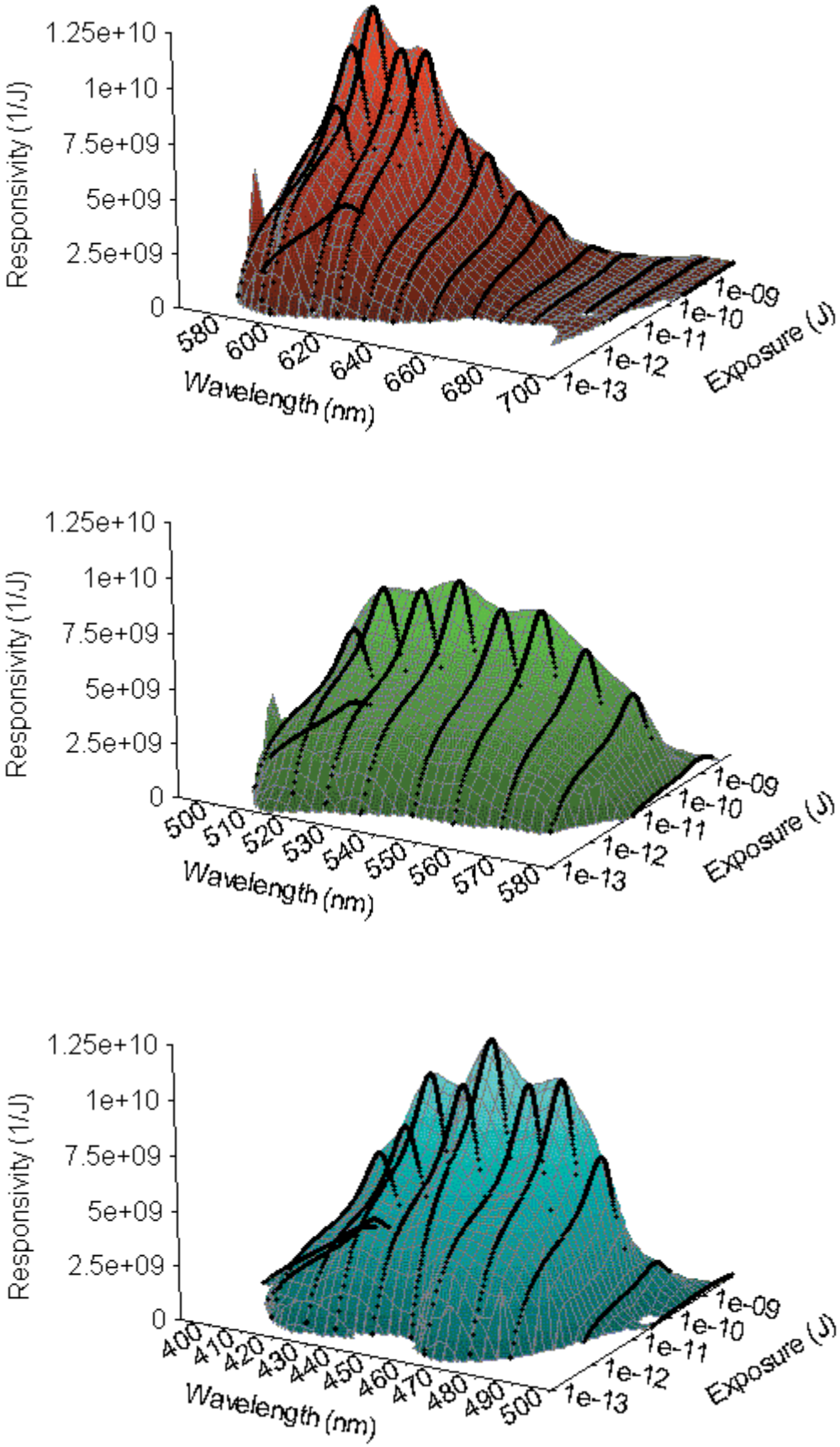

Color Plate 7. 3–D spectral responsivities of RGB channels of a Sony DXC–930P video camera plus a Matrox AT–850 grabber. The solid lines are the spectral profiles of the responsivity at variable exposure and fixed wavelength. (Top: R channel; center: G channel; bottom: B channel.) (Martínez-Verdú, et al., pp. 15–25)

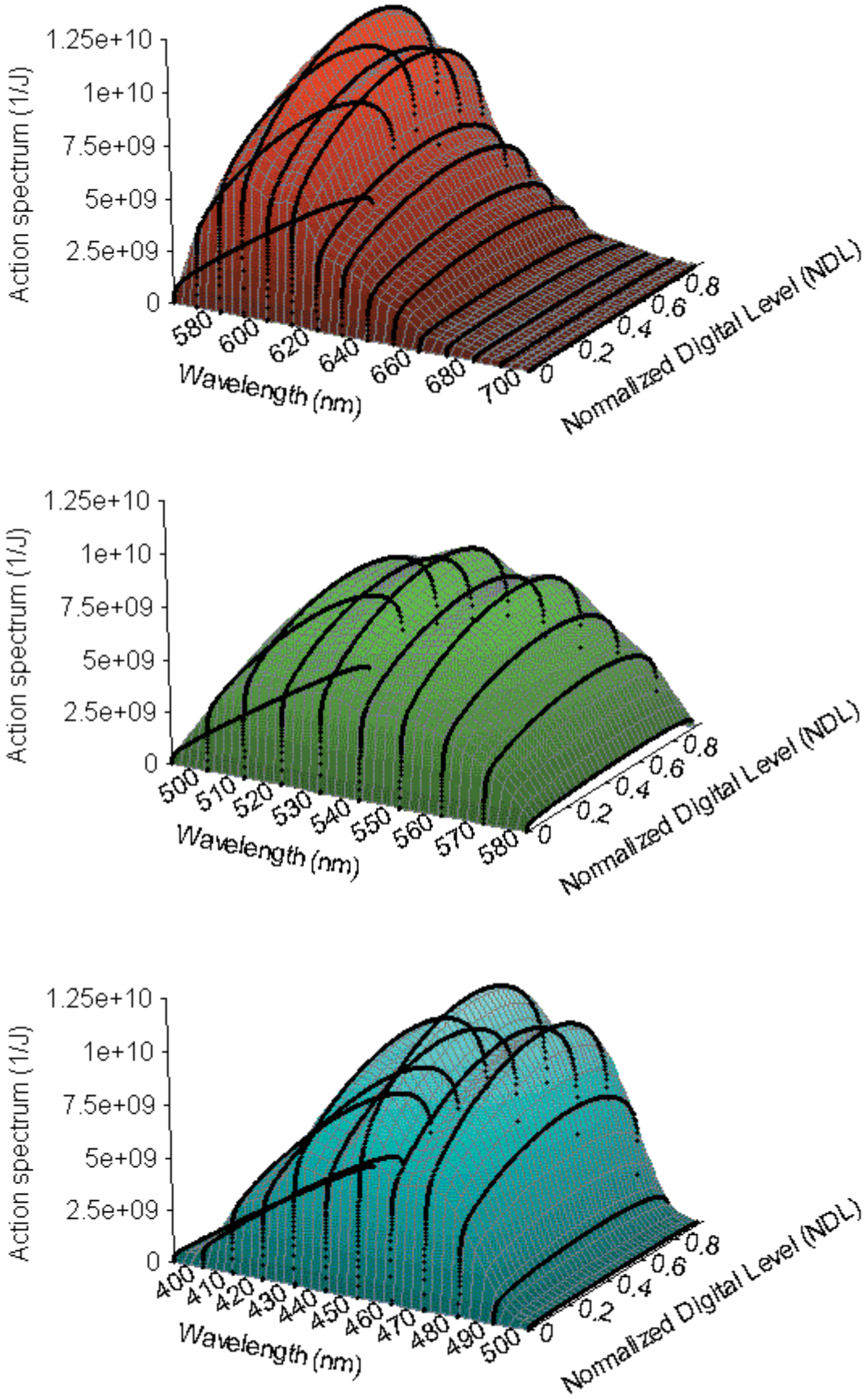

Color Plate 8. 3–D action spectra of the RGB channels of a Sony DXC–930P video camera plus a Matrox AT–850 frame grabber. The solid lines are the spectral profiles of the action spectrum at variable normalized digital level and fixed wavelength. (Top: R channel; center: G channel; bottom: B channel.) (Martínez-Verdú, et al., pp. 15–25)

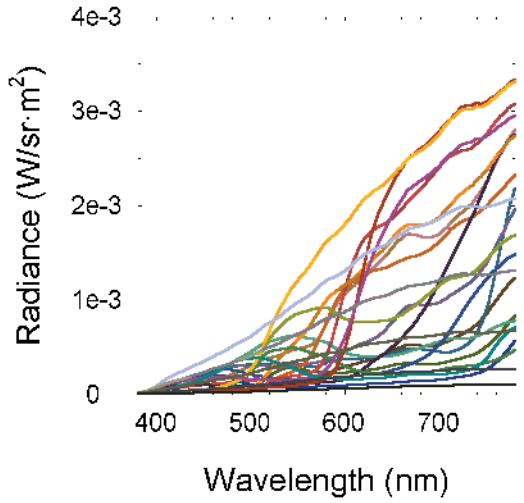

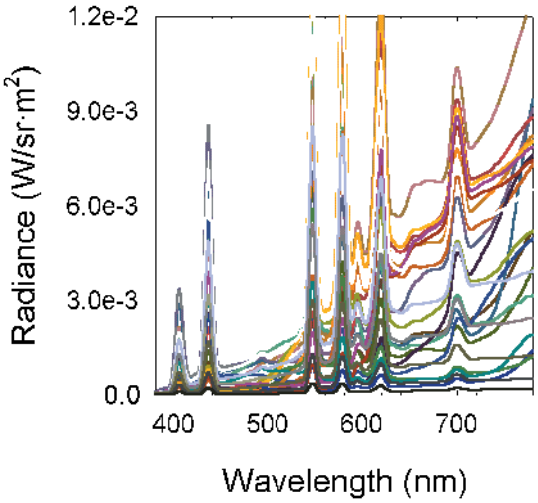

Color Plate 9. Above: Color-stimuli of the Macbeth Color-Checker Chart under incandescent light source (INC lamp). Bottom: Simulation of the image captured by our digital image capture device. (Martínez-Verdú, et al., pp. 15–25)

Color Plate 10. Above: Color-stimuli of the Macbeth Color-Checker Chart under incandescent metal halide light source (HWL lamp). Bottom: Simulation of the image captured by our digital image capture device. (Martínez-Verdú, et al., pp. 15–25)

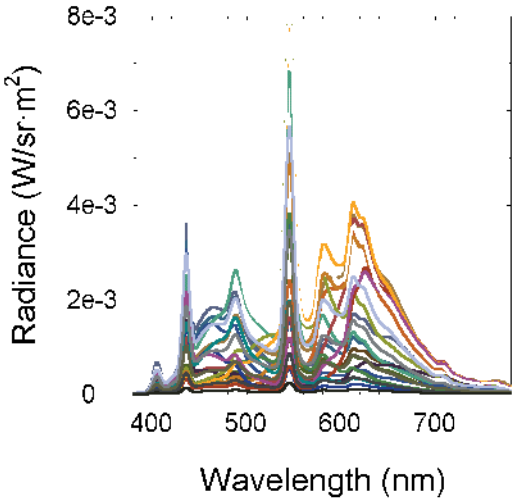

Color Plate 11. Left: Color-stimuli of the Macbeth Color-Checker Chart under fluorescent light source (DAY lamp). Right: Simulation of the image captured by our digital image capture device. (Martínez-Verdú, et al., pp. 15–25)